

Laboratory Gasification Memo

Driving Force Discrimination Experiments

Summary

In order to obtain an understanding if the main driving force for conversion of biomass to syngas is driven by kinetic or heat transfer limitations, an experimental matrix was designed to test different levels of maximum residence time and the maximum possible enthalpy change of the reactants. Experimental results shine light on fundamental driving forces for carbon conversion and tar and methane production in the laboratory gasification system. It was found that the total enthalpy load on the reactor was the primary driving force for carbon conversion, and lower loads led to higher conversions. Changing residence times did not affect carbon yield or carbon release. Finally, both residence time and enthalpy load were found to be significant factors in the production of methane and tars in the laboratory system, and some explanation is given in the text.

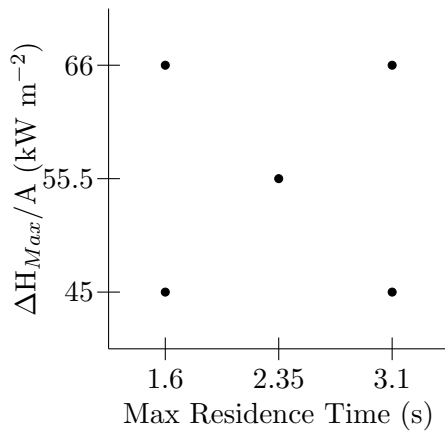


Figure 1: Two factorial experimental matrix used to vary maximum residence time and maximum ΔH between experiments.

Experimental Methods

Design of Experiment

It was desired to create a two factorial matrix with a center point with the two axes representing maximum residence time ($t_{res,max}$) and maximum enthalpy change (ΔH_{max}). The matrix can be seen in Figure 1. Partial pressure of steam and partial pressure of CO₂ were held constant for these experiments at 7 psi and 30 psi, respectively. These pressures were chosen because a large number of previous gasification experiments had partial pressures of CO₂ and H₂O near these values.

Because of the large number of possible set points in the laboratory gasifier system that would effect both the space time and maximum enthalpy simultaneously, it would have been difficult to manually design this experimental matrix. To aid in the design, a large number of potential gasifier experiments were simulated using Sundrop Fuels' gasifier analysis software suite. First, a flow rate of CO₂ was randomly assigned using a uniform distribution with a minimum possible flow rate of 3 SLPM and a maximum flow rate of 6.6 SLPM. The partial pressure of CO₂ was set at 7 psi, and the appropriate flow rate of steam to lead to a partial pressure of 30 psi was found with Equation 1.

$$\dot{n}_{H_2O} = \dot{n}_{CO_2} \times \frac{P_{H_2O}}{P_{CO_2}} \quad (1)$$

The flow rate of Argon was set at 2 SLPM for all experiments. Biomass flow rate was randomized uniformly between 2 lbs/hr and 4 lbs/hr. The total flow rate of entrainment gas was set to be 6 SLPM for every 1 lb/hr of biomass, which was found to be a good minimum entrainment flow rate in previous experiments using the brush feeder. The remainder of the entrainment gas which isn't CO₂ was set as nitrogen.

Steam temperature was set at 500 °C, and makeup nitrogen was uniformly randomized between 0 and 20 SLPM. The total pressure was found using the partial pressure of steam and the total flow rate of gas into the system (Equation



2). The maximum residence time and the maximum enthalpy change were calculated for each simulated run using Sundrop Fuel's gasifier analysis software. Experiments which could not be run due to system limitations were removed from the potential runs, and enthalpy and maximum residence time targets were chosen to maximize the change in each measure. Set points for all experiments are outlined in Appendix F.

$$P_{tot} = P_{H_2O} \times \frac{\dot{n}_{tot}}{\dot{n}_{H_2O}} \quad (2)$$

Calculations

The maximum and minimum residence times are both used for analyses in this memo. Maximum residence time, sometimes referred to as space time, is calculated with Equation 3, which uses the inlet temperature of all reactants going into the reactor to calculate the volumetric flow rate of inlet gas. Minimum residence time, calculated with Equation 4, and uses outlet flow rates and the reactor wall temperature.

$$t_{max} = \frac{VP}{\sum_{i \neq biomass} \dot{n}_i RT_{mix}} \quad (3)$$

$$t_{min} = \frac{VP}{(\sum_{i \neq H_2O} \dot{n}_i + \dot{n}_{H_2O,0}) RT_{wall}} \quad (4)$$

The heat duty is calculated using the maximum possible enthalpy change between the reactants and products assuming complete conversion and the reactor wall temperature in Equation 5.

$$\Delta H_{max} = \sum_{products} n_i \left[\Delta H_i^\circ + \int_{T^\circ}^{T_{out}} C_{p,i} dT \right] - \sum_{reactants} n_i \left[\Delta H_i^\circ + \int_{T^\circ}^{T_{in,i}} C_{p,i} dT \right] \quad (5)$$

Two measures of carbon conversion are discussed in this memo. The first is the fraction of carbon in the biomass which is converted to either CO or CO₂, as these are the two species which are the precursor to synthetic liquid products in the planned commercial process. This measure is referred to as carbon yield, although it

has been referred to in the past as good conversion, and is given in Equation 6.

$$Y_{CO+CO_2} = \frac{\dot{n}_{CO,out} + \dot{n}_{CO_2,out} - \dot{n}_{CO_2,in}}{\dot{n}_{C_{biomass},in}} \quad (6)$$

The second measure is carbon release, which has been referred to in the past as total conversion. This was calculated using Equation 7 and is a representation of the fraction of carbon in the biomass which is converted to any gaseous species detected by the mass spectrometer.

$$X_C = \frac{\dot{n}_{C_{gas},out} - \dot{n}_{CO_2,in}}{\dot{n}_{C_{biomass},in}} \quad (7)$$

Tar loading is a measure of the mass of tars detected by the mass spectrometer (C₆H₆, C₇H₈, and C₁₀H₈) in a standard volume of product gas. This value was calculated using Equation 8.

$$C_{tar} = \frac{\dot{n}_{C_6H_6} + \dot{n}_{C_7H_8} + \dot{n}_{C_{10}H_8}}{\dot{V} \left(\frac{P}{P_{std}} \right) \left(\frac{T_{std}}{T} \right)} \quad (8)$$

Finally, the last measure discussed in this memo is methane yield. It is a representation of the fraction of carbon in the biomass which is converted to methane, and it was calculated using Equation 9. A table defining all variables used in this memo can be found in Appendix H.

$$Y_{CH_4} = \frac{\dot{n}_{CH_4}}{\dot{n}_{C_{biomass},in}} \quad (9)$$

Results and Discussion

Because only inlet conditions of the reactants were needed to calculate the maximum residence time, the experimental matrix was designed based on this calculation. Once experiments were completed and outlet conditions were known, a minimum residence time could be calculated assuming all products reached the wall temperature of the reactor and reacted fully immediately upon entering the reactor. In reality, the actual residence time was somewhere between these boundaries, and the actual residence time would be very difficult to estimate with the data known from the experiments.



Table 1: ANOVA results on effects of designed experimental campaign for carbon yield.

Effect	Prob <F	
	1350 °C	1450 °C
$t_{res,min}$	0.1845	0.0059
$\Delta H_{Max}/A$	<0.0001	0.0002
$t_{res,min} \times \Delta H_{Max}/A$	0.5060	0.9646

Plotted results are shown in Appendices A, B, C, and D for carbon yield, carbon release, tar loading, and methane yield using both the maximum and minimum residence times for visualization purposes. ANOVA results are shown using only minimum residence time. While the magnitude of the effects may be slightly different when using either minimum or maximum residence time, the time chosen for analysis does not change which factors are shown to be statistically significant when using ANOVA.

Carbon Yield

Carbon yield results are plotted in Figures 2, 3, 4, and 5 in Appendix A. ANOVA results are given in Table 1, and factors which had a statistically significant effect on carbon yield are highlighted in red. At 1350 °C, minimum residence time was not statistically significant while $\Delta H_{Max}/A$ was. Both minimum residence time and $\Delta H_{Max}/A$ were statistically significant at 1450 °C. However, as shown in the aforementioned plots, higher residence times led to lower carbon yields, if there was an effect. Since it is very unlikely that the reaction would proceed backwards and lead to lower conversions at longer residence times, it's likely that the effect did not exist, or that another factor was correlated with the changing residence times that is causing the difference in calculated carbon yields. Further tests may be held in the future holding different factors constant to see what is actually driving the variance.

Carbon Release

Carbon release results are plotted in Figures 6, 7, 8, and 9 in Appendix B. Results from ANOVA,

Table 2: ANOVA results on effects of designed experimental campaign for carbon release.

Effect	Prob <F	
	1350 °C	1450 °C
$t_{res,min}$	0.1175	0.0017
$\Delta H_{Max}/A$	0.0005	0.0002
$t_{res,min} \times \Delta H_{Max}/A$	0.8289	0.7615

Table 3: ANOVA results on effects of designed experimental campaign for tar loading.

Effect	Prob <F	
	1350 °C	1450 °C
$t_{res,min}$	<0.0001	0.0654
$\Delta H_{Max}/A$	0.0015	0.8029
$t_{res,min} \times \Delta H_{Max}/A$	0.0002	0.2309

shown in Table 2 reflected what was seen in carbon yield measurements. The total maximum enthalpy load was a significant factor in the carbon release at both 1450 °C and 1350 °C. Again, while minimum residence time was statistically significant at 1450 °C, longer residence times actually gave lower conversions. Since this result contradicts kinetic considerations, further tests may be completed in the future to see if some other factor correlated with the changing residence times was causing the apparent dependency of conversion on residence time.

Tar Loading

Figures 10, 11, 12, and 13 in Appendix C show the results for tar loading values from each experiment in the campaign. Longer residence times and lower enthalpy loads appear to have led to lower tars at 1350 °C. ANOVA results shown in Table 3 show that both residence time and $\Delta H_{Max}/A$ had statistically significant effects on the amount of tars produced at 1350 °C, but not at 1450 °C. This is similar to past results at 1450 °C where the tar levels were on the same order of magnitude as the variance between runs, so conclusions about difference in tar levels cannot be made.



It is important to note that residence time had a significant effect on tar loading at 1350 °C, but it did not have a significant effect on conversion measures at this temperature. There is a reasonable physical explanation for this. While the reactions that contribute to the conversion measures span the entire temperature range (280 °C to 1300 °C), those that are involved in refractory tar cracking do not have measureable rates until the gas reaches 900 °C or 1000 °. Due to the exponential relationship of reaction kinetics to temperature, most of the reactions contributing to the carbon yield and carbon release figures would have very high rates at temperatures where the rate of tar cracking would be low. As these lower temperature reactions are endothermic, they would realistically need to complete themselves before the temperature was able to achieve conditions where tar cracking was important. Indeed, it is the exponential dependence of kinetics on temperature that is the reason for the heat transfer limitation – if heat transfer is not limiting, the temperature of a fluid parcel would rise until it either was the limiting factor or the parcel was at the wall temperature. If the heat transfer were to be greatly reduced near the exit of the furnace (either due to a lower driving force (ΔT) or a reduced number of radiation absorbers), the temperature could hover in the range where kinetic limitations were important for tar cracking.

The experimental evidence does suggest this. The tar levels decrease both with residence time and with heat duty. If it were kinetics alone and the material were close to the wall temperature, only residence time would matter. The dependence on heat duty suggests that exit temperature is important in determining the final level of tars in the system. From a reactor development perspective, there are two pathways that could be chosen to reduce the impurity level. The first would be to increase residence time. However, this would restrict one to the kinetic rate curve at the temperature determined by the slowed rate of heat transfer. The second would be to improve heat transfer. This would have the advantage of increasing the temperature, greatly improving the kinetic rates and reducing the residence time

Table 4: ANOVA results on effects of designed experimental campaign for methane yield.

Effect	Prob <F	
	1350 °C	1450 °C
$t_{res,min}$	<0.0001	0.0001
$\Delta H_{Max}/A$	<0.0001	0.0065
$t_{res,min} \times \Delta H_{Max}/A$	0.0009	0.1305

requirements for cracking. As the major conversion curves only depend on heat duty and improving heat transfer does have an effect on the impurity level, it is recommended that the focus be on heat transfer improvement.

Methane Yield

Methane yield showed similar results as tar loading. Results are shown in Figures 14, 15, 16, and 17 in Appendix D. ANOVA results, shown in Table 4, show that both residence time and $\Delta H_{Max}/A$ were statistically significant for methane yield at 1350 °C as well as 1450 °C. Longer space times and lower enthalpy loads led to lower methane yields at both temperatures.

As with the tar cracking reactions, methane cracking reactions do not have appreciable rates until very high temperatures (>1100 °C). For many of the same reasons described above, the dual dependence on heat duty and residence time is likely a very tight balance between limiting heat transfer and energy consumption by reaction. If the rate of heat transfer could be improved, the system temperature would rise until a new equilibrium was established at a higher temperature where the reaction rates were much faster. Previous experimentation and kinetic models showed that exit temperatures of 1200 °C to 1250 °C would be sufficient to remove essentially all methane. The fact that the dependence on either residence time or heat duty is essentially eliminated at 1450 °C suggests that at the higher temperature the additional driving force is enough to lift temperatures above the threshold for fast cracking.



Normalized Heat Duty

One good test to see if the carbon conversions are driven by heat transfer is to normalize the heat duty by dividing it by the temperature of the reactor wall to the fourth power. Since previous heat transfer tests have shown that the actual wall temperature is about 50 °C lower than what is measured by the skin thermocouples during normal operation, the temperatures were lowered by 50 °C. Graphs showing carbon yield and carbon release plotted against this normalized heat duty are found in Appendix E in Figures 18 and 19.

For carbon yield, the data collapses together a little bit, and begins to form a single function for both 1350 and 1450 °C data. This indicates that the heat duty had a large role in the carbon yield, but there were other factors playing a role in this measure. This could be because the heat duty normalization does not take convection into account. The carbon release, on the other hand, appears to line up between 1350 °C and 1450 °C very well. These two plots show that the heat transfer from radiation is a primary driving force in the laboratory gasifier, but it was not the sole driving force for these experiments.

Conclusion

Experiments showed that residence time did not have an effect on carbon conversion. While res-

idence time showed a statistically significant effect on carbon yield and carbon release at 1450 °C, the effect is opposite of what has been observed in the past and may be due to another untested factor correlated with residence time in the experimental design. There was no statistically significant effect of residence time on either measure of conversion at 1350 °C. Heat duty, on the other hand, had a significant effect on carbon conversion at both temperatures.

Residence time did, however, have an effect on tar loading at 1350 °C and methane yield at both 1350 °C and 1450 °C. Longer times led to lower amount of the undesired products. Effects that enthalpy load had on tar and methane production mirrored those displayed by residence time.

Future experiments should be completed which will hold different factors constant throughout the experimental campaign. Additionally, the conversions seen for given enthalpy loads are lower than previous gasification experiments. The biomass used in these experiments is from a different production run. Experiments will be completed in the near future that repeat previous experimental set points with the new biomass to compare the results with old biomass. If results come back with different conversions, then old biomass will be used under the same conditions to see if there has been a change in the system recently.



A Carbon Yield Plots

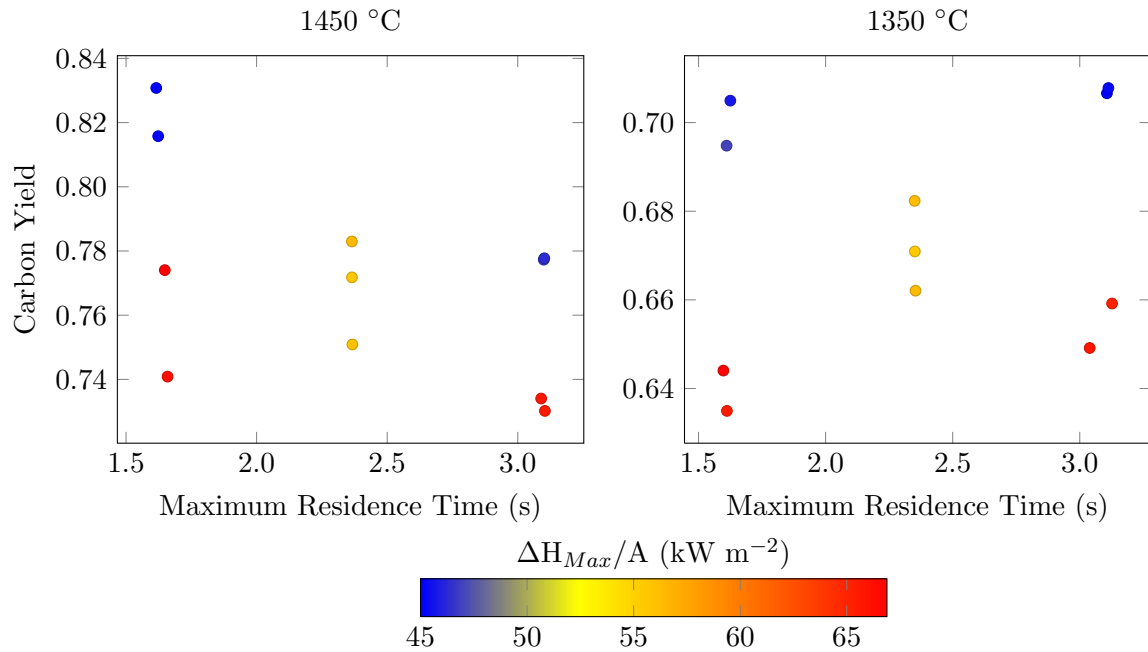


Figure 2: Results for carbon yield plotted against maximum residence time and colored by enthalpy load. At 1450 °C, longer space times actually lead to lower conversions for similar enthalpy loads. At 1350 °C, the difference in conversions at different space times but similar enthalpy loads is close to the variance between replicates, and ANOVA results show that residence time has no effect on carbon yield.

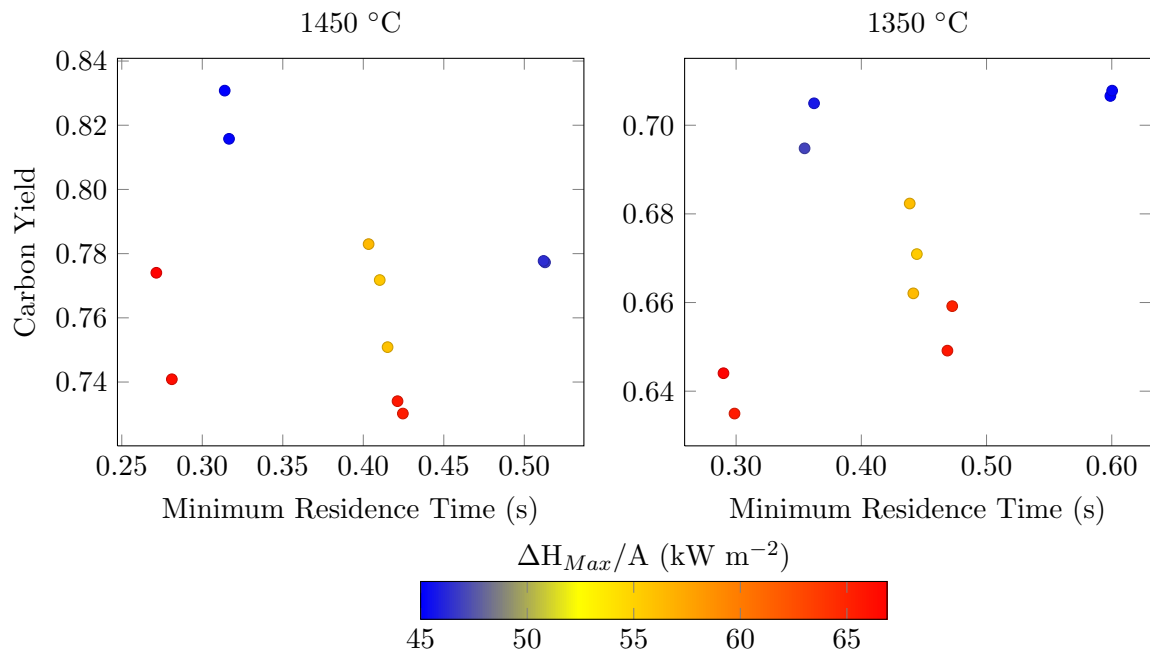


Figure 3: Carbon yield is plotted against minimum residence time rather than maximum residence time. Although data points are shifted across the x-axis relative to each other, the same conclusions are reached when looking at minimum residence time rather than maximum residence time.

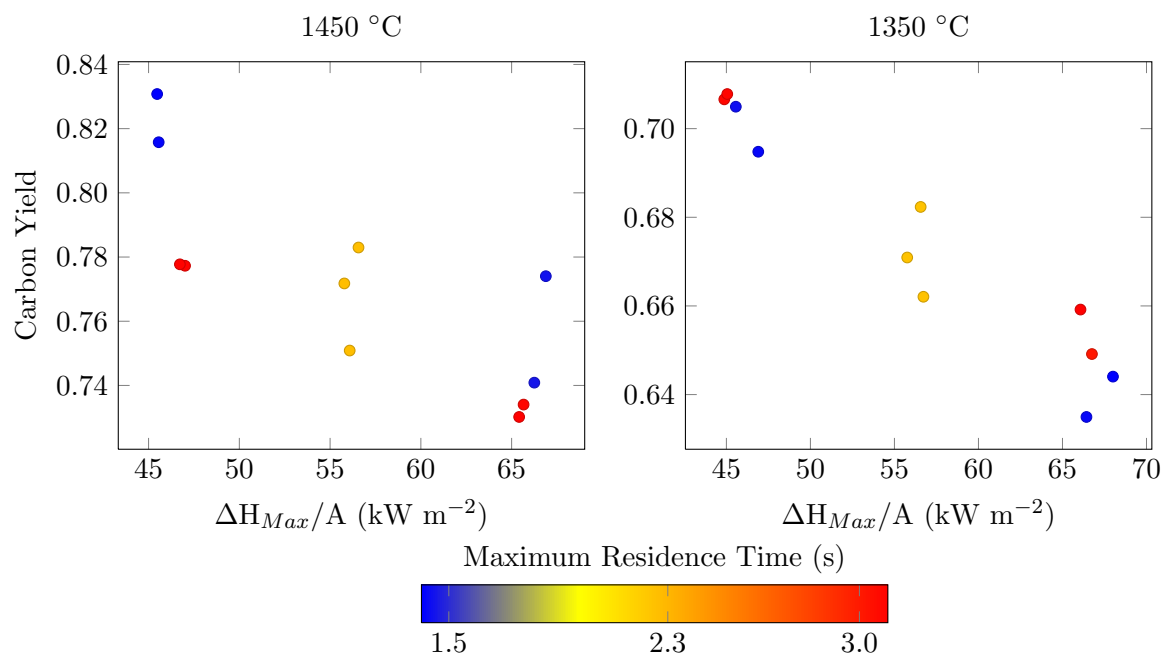


Figure 4: Here, carbon yield is plotted against $\Delta H_{Max}/A$. At 1450 °C, it appears as though lower residence times lead to higher conversions, which is counter-intuitive. At 1350 °C, the conversions at different residence times collapse onto each other, and it is easy to see the lack of effect that residence time has on carbon yield.

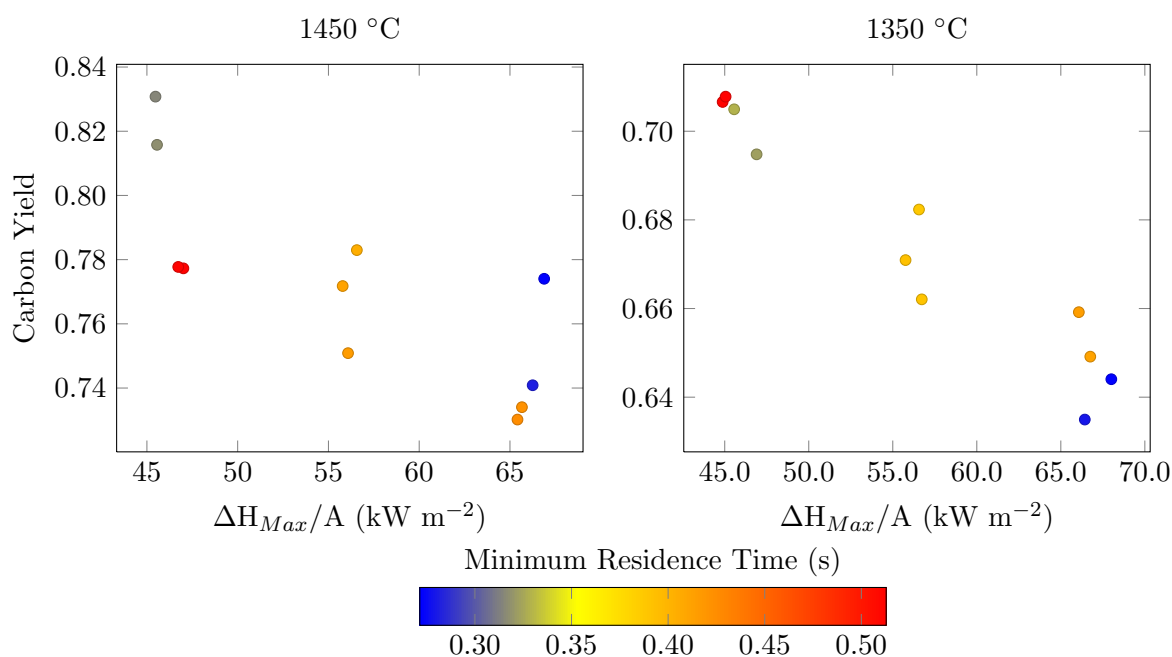


Figure 5: Carbon yield is plotted against $\Delta H_{Max}/A$ and colored according to minimum residence time. Again, the same conclusions are met no matter if minimum or maximum residence time is used for analysis.



B Carbon Release Plots

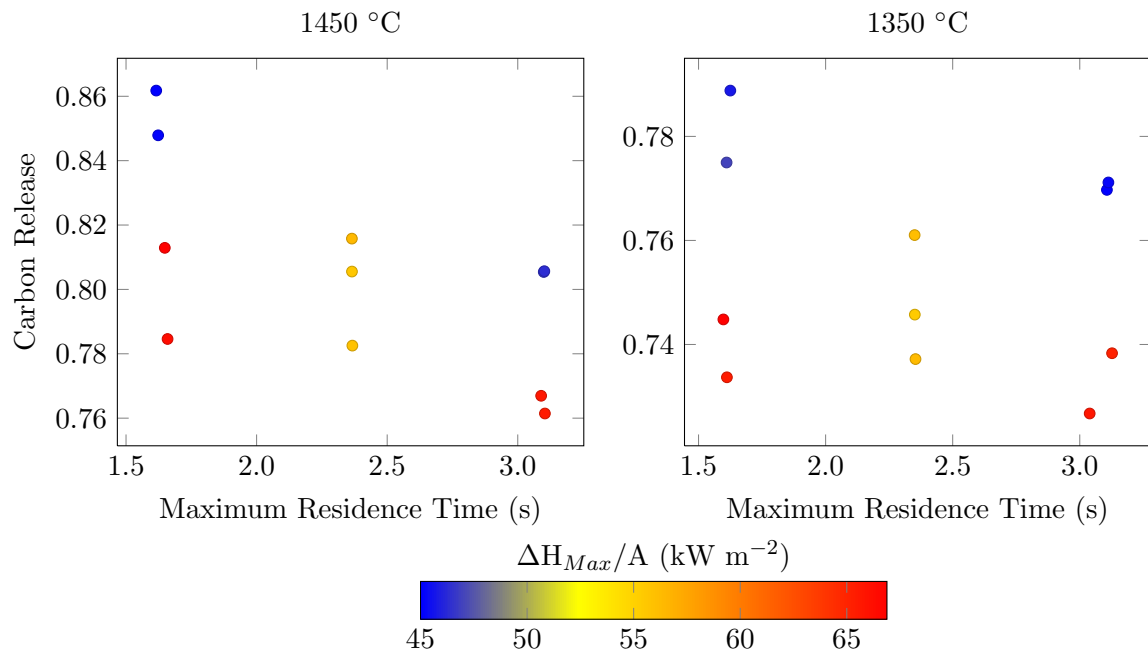


Figure 6: Carbon release results show the same trends as carbon yield, but the difference in carbon release for similar residence times and different enthalpy loads are slightly larger than they were for carbon yield. At 1450 °C, maximum residence time shows a negative effect on conversion and has no effect on conversion at 1350 °C.

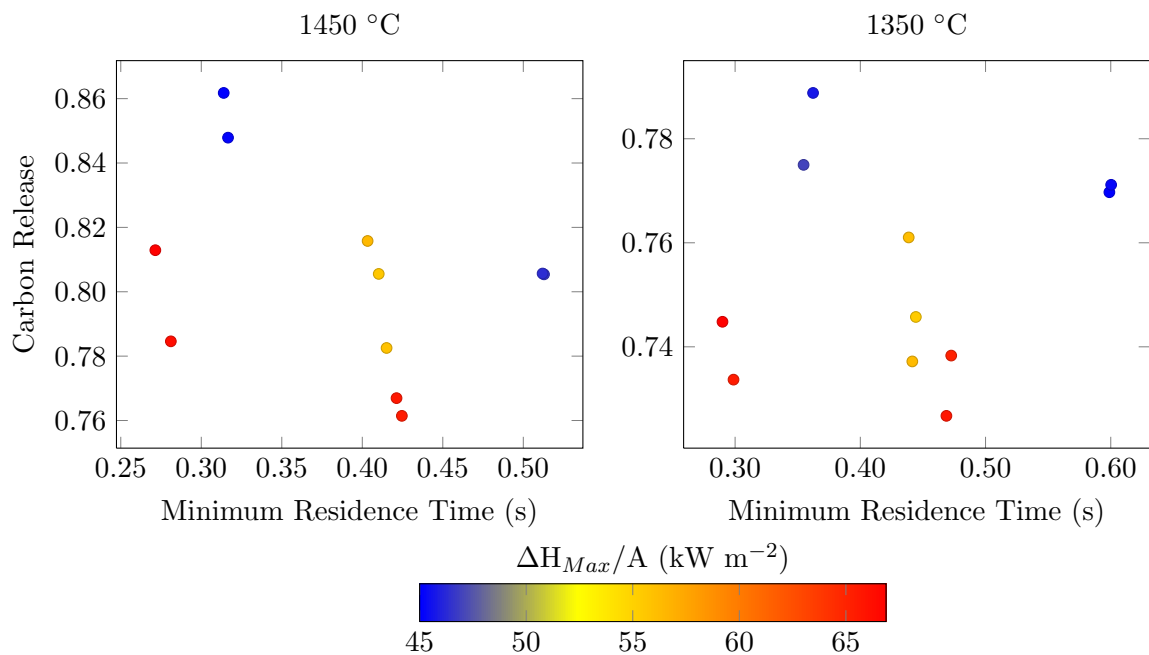


Figure 7: Carbon release versus minimum residence time colored by enthalpy load.

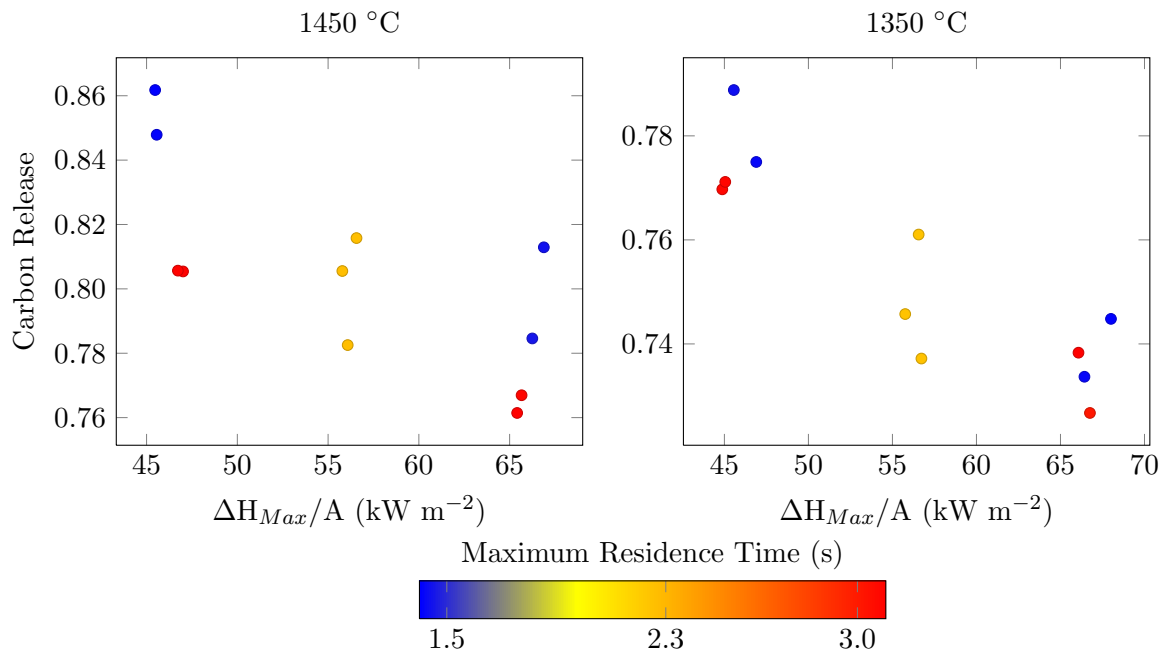


Figure 8: Carbon release plotted against enthalpy load clearly shows dependence that carbon release has on $\Delta H_{Max}/A$ at both temperatures.

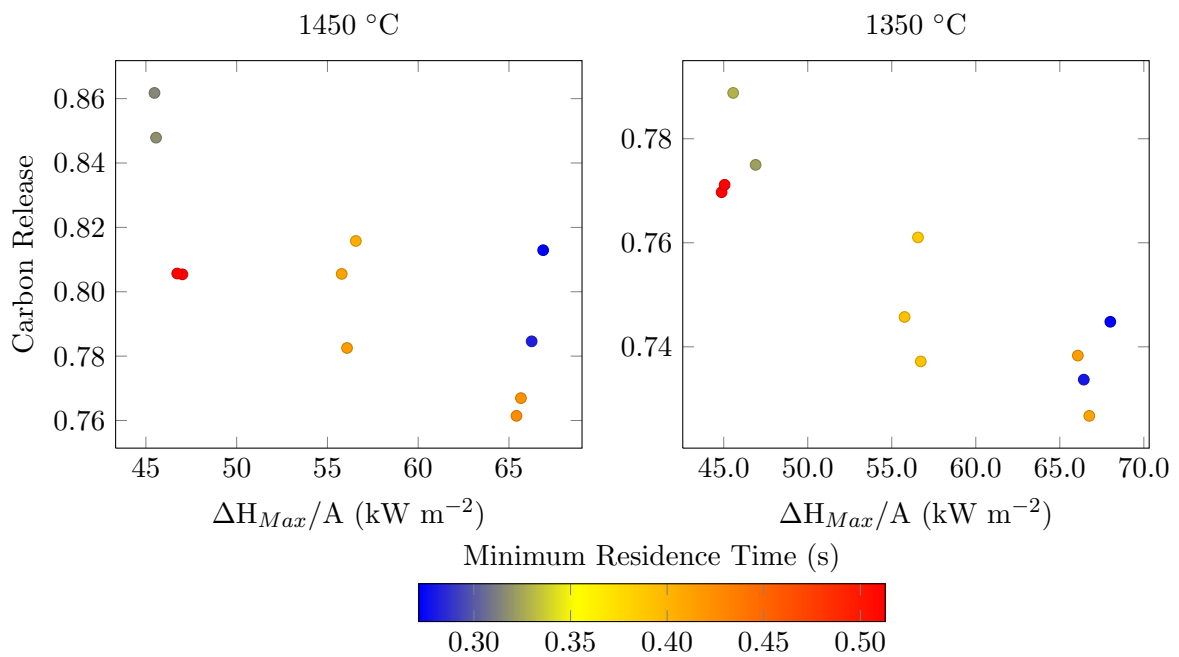


Figure 9: Carbon release versus $\Delta H_{Max}/A$ colored according to minimum residence time.



C Tar Loading Plots

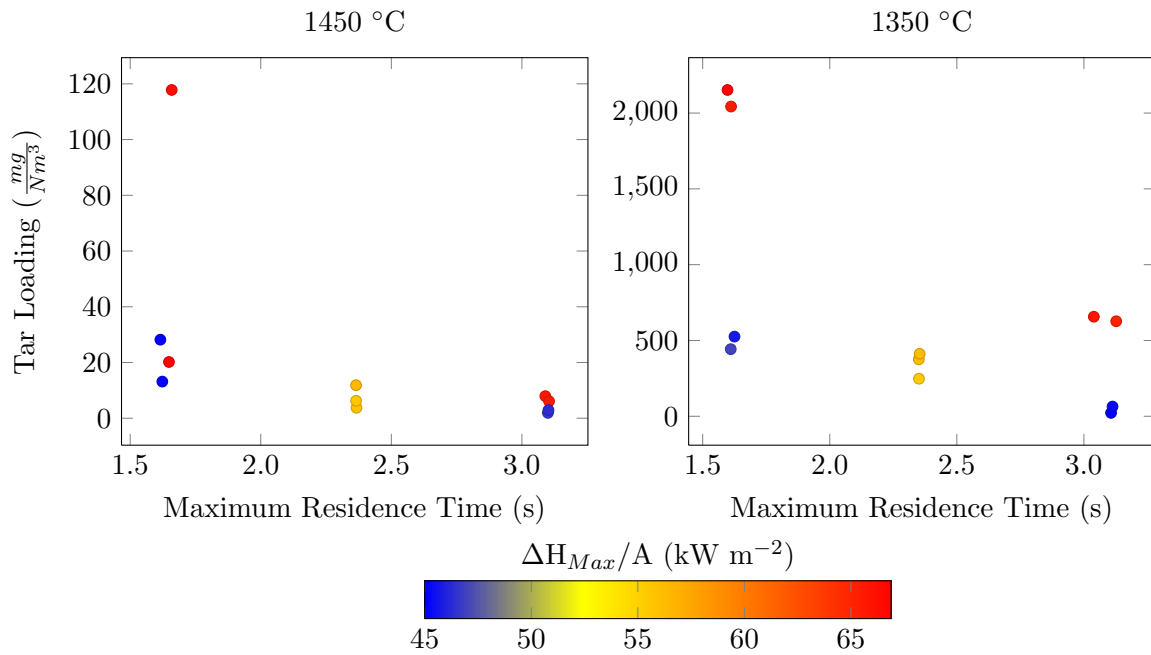


Figure 10: Tar loading results plotted against maximum residence time. Tar levels at 1450 °C are too low to see any effects that residence time or enthalpy load may have on tar make. At 1350 °C, there are effects from both factors. Lower tar loads are a result of longer space times and lower enthalpy loads.

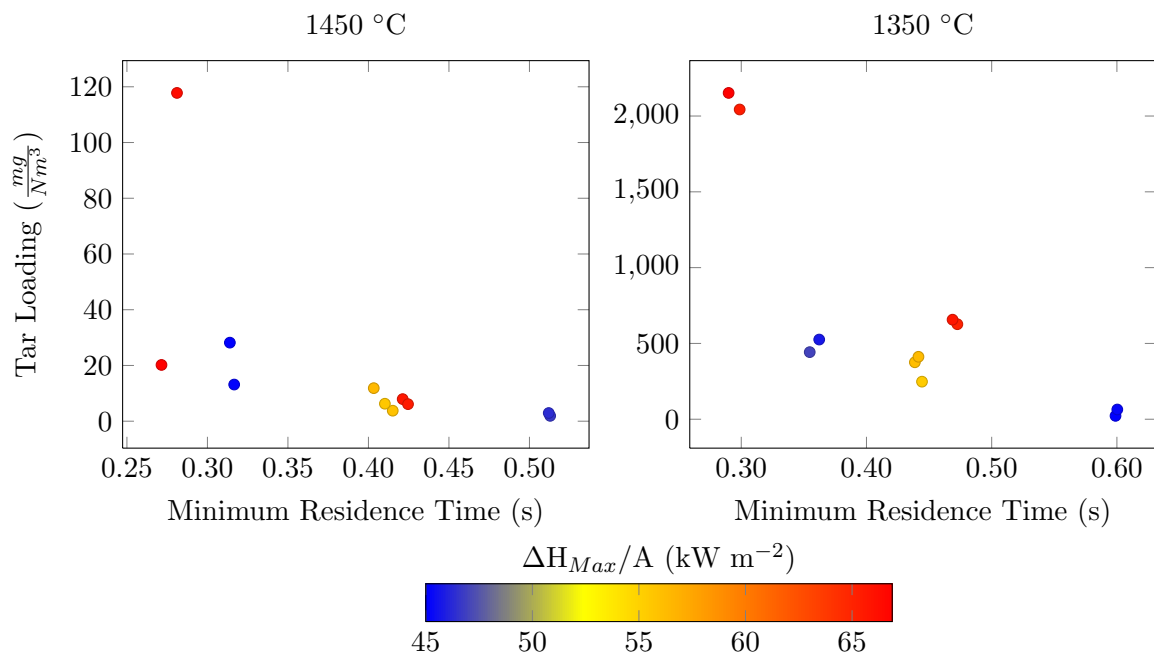


Figure 11: Tar loading versus minimum residence time colored by enthalpy load.

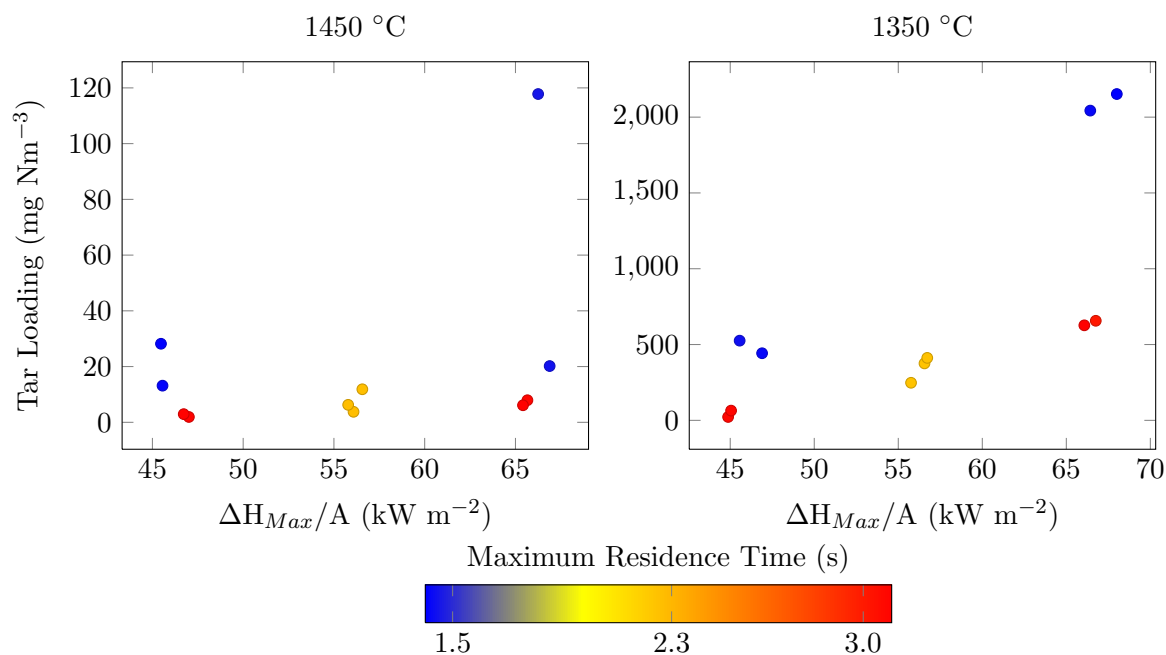


Figure 12: Tar loading versus enthalpy load colored according to maximum residence time.

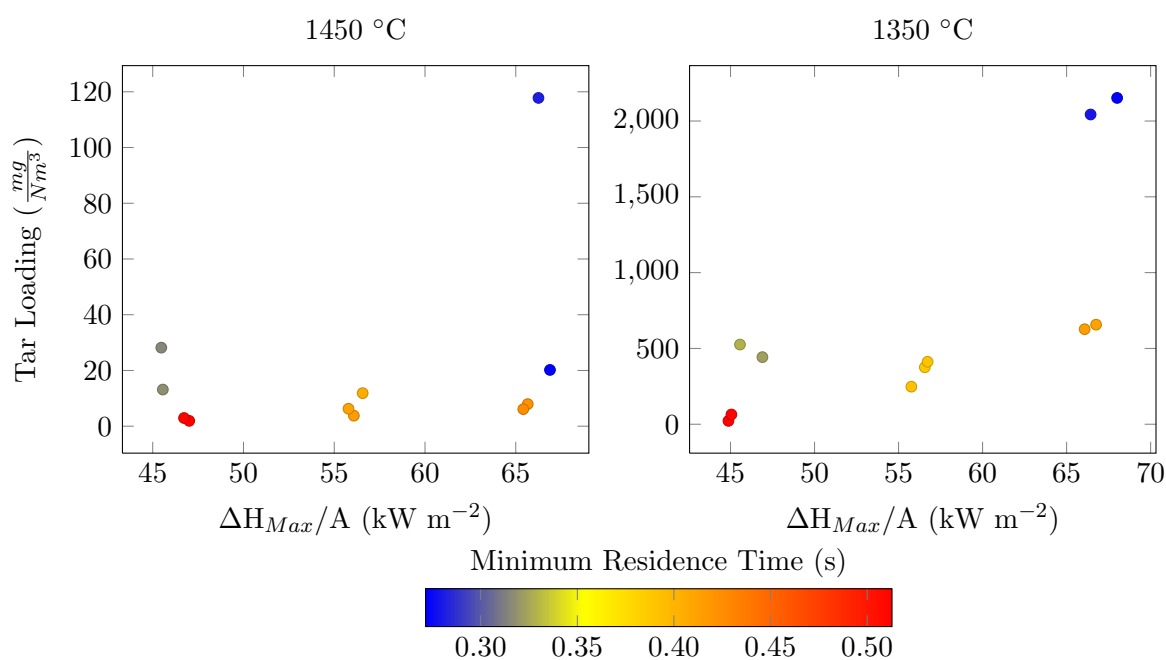


Figure 13: Tar loading plotted against $\Delta H_{Max}/A$ and colored by minimum residence time.



D Methane Yield Plots

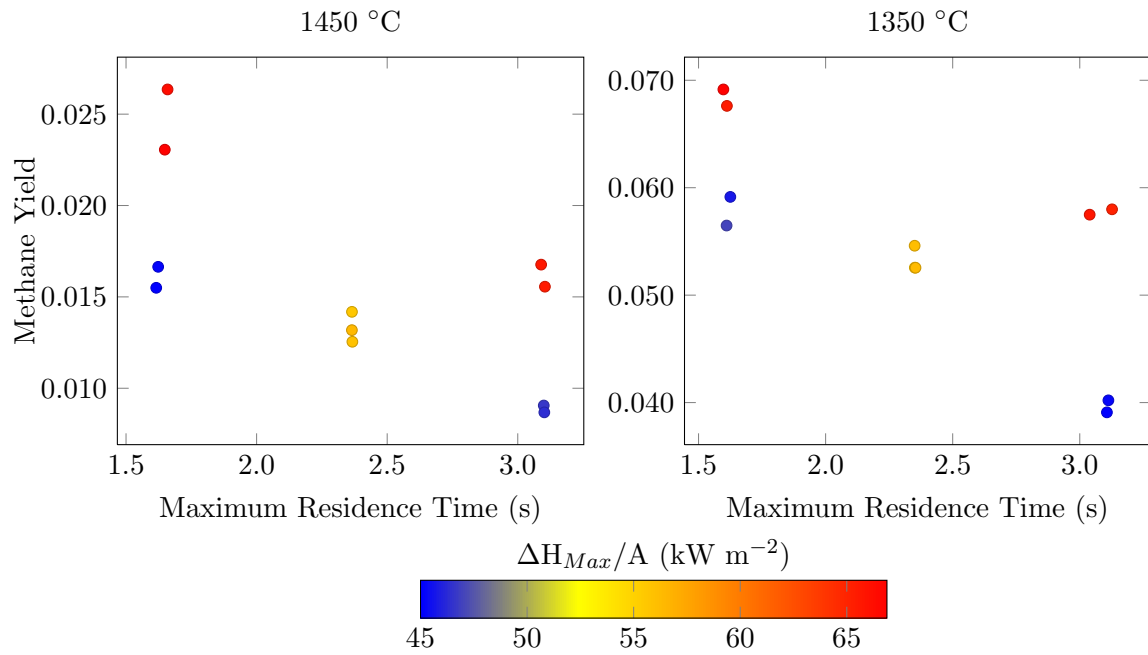


Figure 14: This plot showing methane yield vs. maximum residence time shows that there are effects on methane yield from both residence time and heat duty at both sets of temperatures.

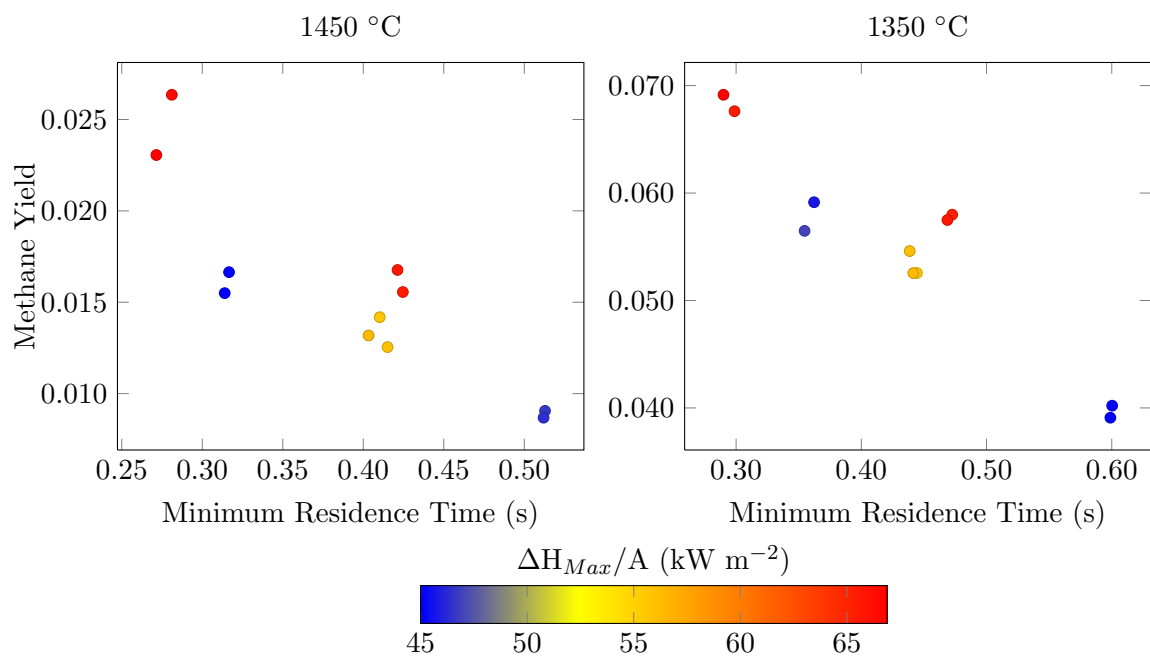


Figure 15: Methane yield plotted against minimum residence times shows a strong dependence on the minimum residence time.

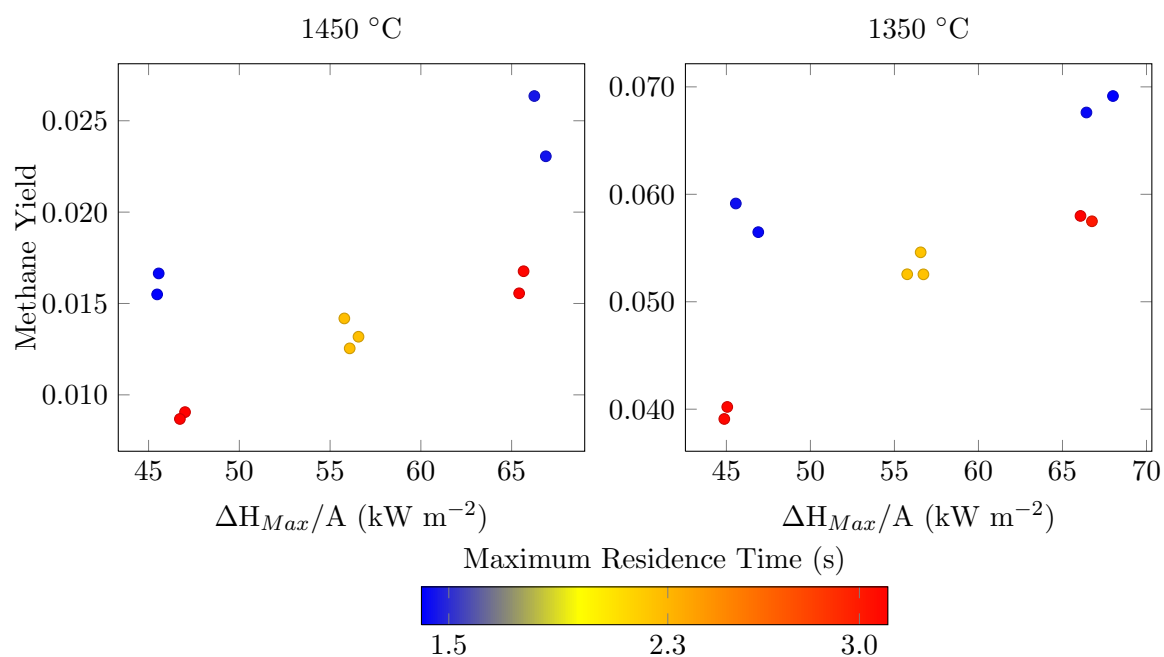


Figure 16: Methane yield plotted against $\Delta H_{Max}/A$ and colored by maximum residence time.

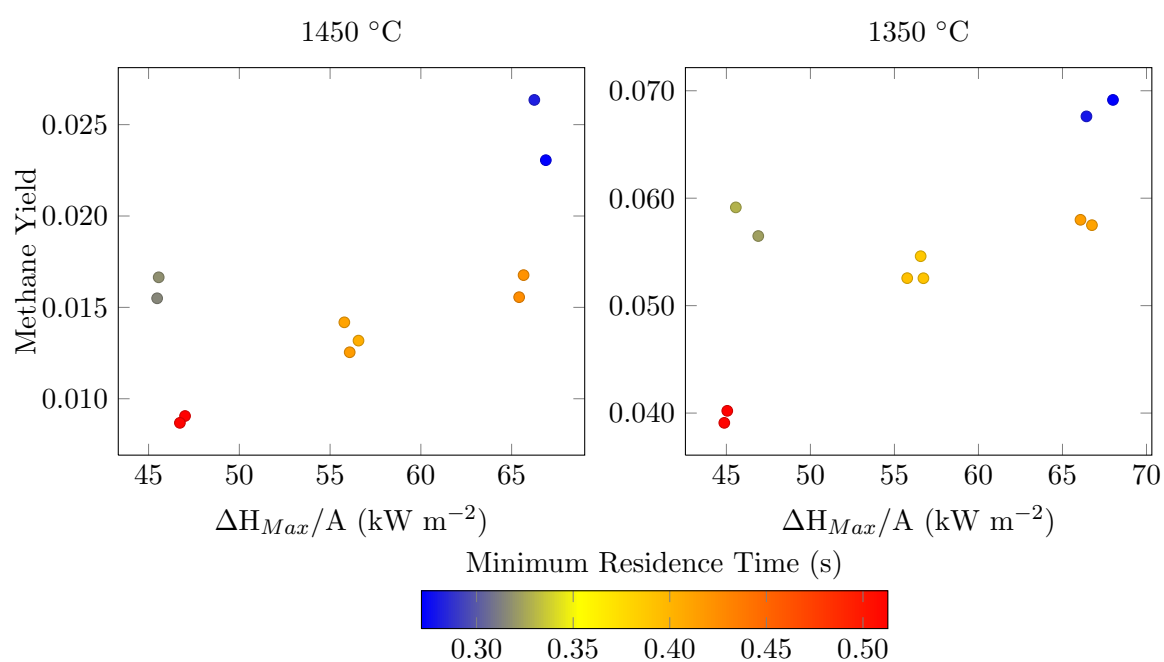


Figure 17: Methane yield plotted against $\Delta H_{Max}/A$ and colored by minimum residence time.

E Temperature Normalized Heat Duty Plots

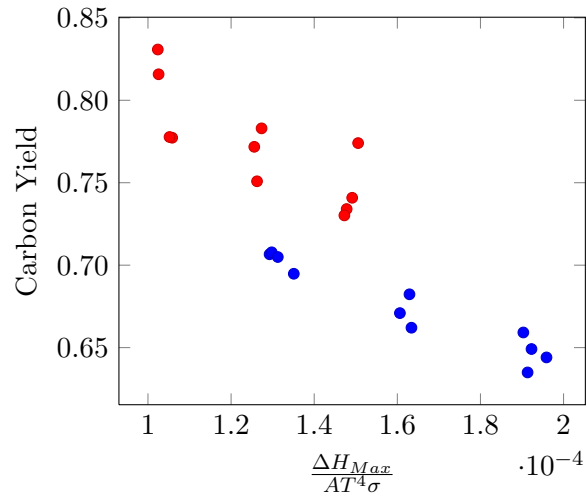


Figure 18: Carbon yield is plotted against the heat duty which has been normalized by the temperature of the reactor wall to the fourth power.

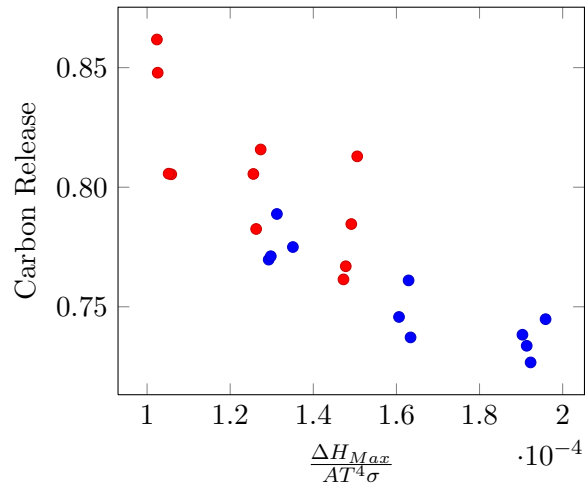


Figure 19: Carbon release is plotted against the heat duty which has been normalized by the temperature of the reactor wall to the fourth power.



F Experimental Set Points

Table 5: Setpoints for enthalpy vs. space time experiments. Steam temperature is at 500 °C for all runs, and argon flow is 2 SLPM.

Target $\Delta H_{max}/A$ (kW m ⁻²)	Target Max Res Time (s)	Temp. (°C)	Biomass (lb/hr)	Ent. N ₂ (SLPM)	Ent. CO ₂ (SLPM)	Makeup N ₂ (SLPM)	Steam (g/min)	Pres- sure (psig)
45	1.6	1450	2.1	6.7	6.0	1.4	19.3	34
45	3.1	1450	2.2	9.3	3.8	11.1	12.0	64
55.5	2.35	1450	2.6	10.5	4.9	14.4	15.7	61
66	1.6	1450	3.5	14.3	6.4	0	20.3	41
66	3.1	1450	3.6	17.9	3.8	4.5	12.2	67
45	1.6	1350	2.1	6.3	6.3	7.9	20.2	40
45	3.1	1350	2.0	8.3	3.9	19.1	12.6	75
55.5	2.35	1350	2.8	11.6	4.9	14.5	15.8	62
66	1.6	1350	3.7	15.6	6.4	1	20.6	42
66	3.1	1350	3.8	18.9	3.9	7.0	12.5	72

G Experimental Results

Table 6: Selected results from the experimental campaign.

Run ID	Temp. (°C)	Max Res Time (s)	Min Res Time (s)	$\Delta H_{max}/A$ (kW m ⁻²)	Carbon Yield	Carbon Release	Tar Loading (mg Nm ⁻³)	CH ₄ Yield
515	1450	1.62	0.314	45.5	0.831	0.862	28.2	0.0155
516	1450	1.66	0.281	66.3	0.741	0.785	118	0.0264
517	1450	3.09	0.421	65.7	0.734	0.767	7.93	0.0168
518	1450	1.65	0.271	66.9	0.774	0.813	20.2	0.0231
519	1450	2.36	0.403	56.6	0.783	0.816	11.9	0.0132
520	1450	3.10	0.425	65.4	0.730	0.761	6.12	0.0156
521	1450	2.37	0.415	56.1	0.751	0.783	3.77	0.0125
522	1450	1.62	0.317	45.6	0.816	0.848	13.1	0.0166
523	1450	3.10	0.513	47.0	0.777	0.805	1.92	0.0091
524	1450	2.37	0.410	55.8	0.772	0.806	6.27	0.0142
525	1450	3.10	0.512	46.7	0.778	0.806	2.93	0.0087
526	1350	3.11	0.599	44.9	0.707	0.770	22.3	0.0391
527	1350	3.04	0.469	66.8	0.649	0.727	657	0.0575
528	1350	2.35	0.444	55.8	0.671	0.746	248	0.0526
529	1350	3.13	0.473	66.1	0.659	0.738	627	0.0580
530	1350	1.60	0.290	68.0	0.644	0.745	2150	0.0691
531	1350	2.35	0.439	56.6	0.682	0.761	376	0.0546
532	1350	1.61	0.299	66.4	0.635	0.734	2040	0.0676
533	1350	1.61	0.355	46.9	0.695	0.775	443	0.0565
534	1350	3.11	0.600	45.1	0.708	0.771	64.1	0.0402
535	1350	1.63	0.362	45.6	0.705	0.789	526	0.0591
536	1350	2.35	0.442	56.7	0.662	0.737	412	0.0526



H Variable Legend

Table 7

Variable	Definition
A	Surface area of the inside surface of the reactor tube
C_{tar}	Tar loading in the product gas in mg Nm^{-3}
ΔH_{max}	Maximum enthalpy change of the reactants assuming complete conversion
$\dot{m}_{i,out}$	Mass flow rate of specie i flowing out of the reactor
$\dot{n}_{C_{biomass},in}$	Molar flow rate of carbon in the biomass flowing into the reactor
$\dot{n}_{C_{gas},out}$	Molar flow rate of carbon in all gaseous species flowing out of the reactor
$\dot{n}_{i,in}$	Molar flow rate of gaseous species i into the reactor
$\dot{n}_{i,out}$	Molar flow rate of gaseous species i out of the reactor
P	Pressure
P_i	Partial pressure of specie i
P_{std}	Standard pressure
T	Temperature
T_{std}	Standard temperature
$t_{res,max}$	Maximum residence time, or space time
$t_{res,min}$	Minimum possible residence time
\dot{V}	Volumetric flow rate
X_C	Carbon release from carbon in the biomass
Y_{CH_4}	Methane yield from carbon in the biomass
Y_{CO+CO_2}	Carbon yield to CO and CO ₂ from carbon in the biomass